

The Disulfide-bonded Loop of Chromogranins, Which Is Essential for Sorting to Secretory Granules, Mediates Homodimerization*

(Received for publication, August 1, 1997, and in revised form, September 29, 1997)

Christoph Thiele‡ and Wieland B. Huttner§

From the Department of Neurobiology, University of Heidelberg, Im Neuenheimer Feld 364, D-69120 Heidelberg, Germany

Chromogranins A and B, two widespread neuroendocrine secretory proteins, contain a homologous N-terminal disulfide-bonded loop that is required for sorting to secretory granules. Here we have investigated the role of this loop in the oligomerization of chromogranin A. Reduction of the disulfide bond or the addition of an excess of an N-terminal chromogranin A fragment containing the loop (CgA₁₋₆₀) resulted in the dissociation into monomers of the chromogranin A dimer found at pH 7.4 and 6.4 and of the chromogranin tetramer found at pH 5.4. The addition of an excess of a synthetic peptide corresponding to the conserved C-terminal domain of chromogranin A (CgA₄₀₆₋₄₃₁) had no effect on the chromogranin dimers at pH 7.4 and 6.4 and resulted in the dissociation of the chromogranin A tetramers at pH 5.4 into dimers. Fluorescence energy transfer experiments using fluorescently labeled CgA₁₋₆₀ showed that the N-terminal disulfide-bonded loop has a high affinity for homodimerization ($K_D = 20$ nM at pH 6.4), which was sufficient to mediate dimerization of full-length chromogranin A. Association and dissociation of loop-mediated chromogranin A dimerization approached completion within a few seconds. Our results imply that chromogranin A homodimerizes shortly after synthesis in the endoplasmic reticulum and that the loop-mediated homodimeric state is an essential prerequisite for its sorting, in the trans-Golgi-network, to secretory granules.

formed, constitutive secretory vesicles and immature secretory granules. In the course of their conversion to mature secretory granules, immature secretory granules give rise to vesicles thought to mediate constitutive-like secretion. Protein sorting takes place at both the level of the TGN and the level of immature secretory granules (1–3).

Concerning the sorting of secretory proteins at the level of the TGN, two important features have been elucidated. One is the selective aggregation of regulated secretory proteins in the lumen of the TGN, which is a means of segregating them from constitutive secretory proteins (4–7). The model proteins in many of these studies have been the granins (chromogranins, secretogranins), a family of regulated secretory proteins that are widespread constituents of neuroendocrine secretory granules (8, 9). Their aggregation is promoted by calcium ions and low pH, two parameters of the TGN luminal milieu (7, 10).

The second feature concerns discrete structures in regulated secretory proteins essential for sorting. N-terminal disulfide-bonded loops have been identified as such structures in chromogranin B (CgB) (11) and pro-opiomelanocortin (12, 13). In the case of pro-opiomelanocortin, the N-terminal disulfide-bonded loop has been shown to bind to the membrane-associated form of carboxypeptidase E (14). This interaction has been implicated in sorting (14, 15), although the claim of an essential role of CPE in sorting is controversial (16).

In the case of CgB, reduction of the disulfide bond is sufficient to cause complete missorting to constitutive secretory vesicles (11). Understanding the molecular mechanism underlying this missorting requires determination whether or not the disulfide-bonded loop participates in an intermolecular interaction and, if so, the identification of the interacting molecule. Chromogranin A (CgA), another member of the granin family, contains an N-terminal disulfide-bonded loop highly homologous to that of CgB (17), which as in the case of CgB is encoded by a separate exon (18–20). Taking advantage of the bovine adrenal medulla as a suitable source for the purification of CgA, we demonstrate here that the disulfide-bonded loop plays the crucial role for oligomerization of CgA, strongly suggesting a link between chromogranin oligomerization and sorting.

MATERIALS AND METHODS

Purification of CgA

All steps were performed at 4 °C. Chromaffin granule pellets, obtained from bovine adrenals as described by Bartlett and Smith (21), were resuspended in a buffer containing 20 mM MES, pH 6.4, 20 mM CaCl₂, 0.5 mM phenylmethylsulfonyl fluoride, and 100 μg/ml leupeptin and lysed by freeze-thawing and sonication. The acidic pH and the high calcium concentration were chosen to maintain CgB, secretogranin II, and other soluble proteins in an aggregated state, while most of the CgA was found to be soluble under these conditions. The lysate was centrifuged at 100,000 × *g* for 30 min, and the supernatant (80 ml, 10 mg/ml

Protein secretion is a fundamental cellular function. Virtually all eukaryotic cells secrete proteins in parallel with their synthesis via the constitutive pathway. Certain cells such as exocrine cells, endocrine cells, and neurons in addition secrete proteins via the regulated pathway; they store a subset of their secretory proteins in a specialized vesicular organelle, the secretory granule, and release them upon appropriate stimulation. The regulated pathway of protein secretion diverges from the constitutive pathway at the level of the trans-Golgi network (TGN)¹, where two distinct types of secretory vesicles are

* The costs of publication of this article were defrayed in part by the payment of page charges. This article must therefore be hereby marked "advertisement" in accordance with 18 U.S.C. Section 1734 solely to indicate this fact.

‡ Supported by a fellowship from the Boehringer-Ingelheim Fonds.

§ Supported by Deutsche Forschungsgemeinschaft Grant SFB 317, C2 by EU-TMR Research Network ERB-FMRX-CT96-0023, and by EU Biotechnology Grant ERB-B104-CT96-0058. To whom correspondence and reprint requests should be addressed. Tel.: 49-6221-548218; Fax: 49-6221-546700.

¹ The abbreviations used are: TGN, trans-Golgi network; CgA, chromogranin A; CgB, chromogranin B; DTT, dithiothreitol; FRET, fluorescence resonance energy transfer; FITC, fluorescein isothiocyanate; TRITC, tetramethylrhodamine isothiocyanate; MES, 4-morpholineethanesulfonic acid; PAGE, polyacrylamide gel electrophoresis; FPLC, fast protein liquid chromatography; BSA, bovine serum albumin;

Tricine, *N*-[2-hydroxy-1,1-bis(hydroxymethyl)ethyl]glycine; FIU, fluorescence intensity units.

protein) was supplemented with 40 mM EDTA and brought to pH 7.4 with NaOH. After extensive dialysis against 50 mM sodium phosphate, pH 7.4, proteins were bound to an anion exchange column (Pharmacia Q-Sepharose, 26 × 100 mm) and eluted using a gradient of 0–1 M NaCl in 50 mM sodium phosphate, pH 7.4. The fractions containing CgA (as determined by SDS-PAGE) were pooled, and CgA was further purified by gel filtration (Superdex 200 HR, 10 × 300 mm, 50 mM sodium phosphate, pH 7.4, 100 mM NaCl, 1 mM EDTA). CgA was concentrated by chromatography on a small anion exchange column (MONO Q, 5 × 50 mm, elution by a gradient of 0–1 M NaCl in 50 mM sodium phosphate, pH 7.4), which typically yielded ~2 ml containing ~10 mg of virtually pure CgA (see top panel of Fig. 2).

Preparation of CgA₁₋₆₀

Unless otherwise indicated, all steps were performed at 4 °C. Chromaffin granule pellets were resuspended in a buffer containing 20 mM MES, pH 6.4, and 20 mM CaCl₂ and lysed by repeated freeze-thawing. The lysate was centrifuged at 200,000 × *g* for 30 min. The supernatant was collected and supplemented with 40 mM EDTA. Following extensive dialysis against 50 mM NH₄HCO₃, pH 7.9, and 1 mM EDTA, the dialyzed solution (80 ml, 5 mg/ml protein) received 200 μg of *S. aureus* V-8 protease. After 2 h of incubation at 37 °C, 3,4-dichloroisocoumarol (100 μl of 10 mg/ml in dimethylformamide) was added to inhibit the protease. The solution was filtered through a 0.2-μm membrane filter and loaded onto an anion exchange column (Q-Sepharose, 26 × 100 mm). The column was washed with 50 mM NH₄HCO₃, pH 7.9, and eluted using a linear 500-ml gradient of 0–1 M NaCl in 50 mM NH₄HCO₃, pH 7.9, and collecting 3-ml fractions upon starting the gradient. Fractions 40–44 (corresponding to the leading shoulder of the first protein peak as determined by the Bradford assay (22)) were pooled, acidified to pH ~2 with trifluoroacetic acid, and subjected to reverse phase chromatography on a Pharmacia PepRPC 15-μm HR 10/10 column, which was eluted using a gradient of 10–90% acetonitrile in 0.1% trifluoroacetic acid. The fractions containing the major protein peak as determined by the Bradford assay were lyophilized and subjected to a second round of reverse phase chromatography. This yielded ~10 mg of peptide, which was found to be >97% pure as determined by densitometric scanning of a Coomassie Blue-stained SDS-polyacrylamide gel. The identity of the peptide as CgA₁₋₆₀ was determined by matrix-assisted laser desorption/ionization mass spectrometry (*m/z* = 6766) and N-terminal sequencing (LPVNSP).

Fluorescent Derivatives of CgA

Purified CgA (1 mg) was dissolved in 900 μl of 50 mM sodium borate, pH 9.0. FITC was added to a final concentration of 1 mM. After incubation for 2 h at room temperature, ethanolamine (1 μl) was added (18.5 mM final concentration). After 30 min of incubation at room temperature, the FITC-CgA was purified by gel filtration (Superdex 200 HR, 10 × 300 mm, 50 mM sodium phosphate, pH 7.4). The stoichiometry of labeling was calculated from the extinction at 494 nm and was found to be 3.5 mol of FITC/mol of CgA. The same protocol was used for labeling of CgA with TRITC (554 nm, stoichiometry of 2.8).

Fluorescent Derivatives of CgA₁₋₆₀

CgA₁₋₆₀ (1 mg/ml in 50 mM sodium borate, pH 9.0) was reacted with 1 mM TRITC for 2 h at room temperature. Ethanolamine was added to a final concentration of 10 mM. After 1 h, the peptide was isolated by gel filtration as above. TRITC-CgA₁₋₆₀ was separated from the unlabeled peptide by reverse phase chromatography as above. Several peaks of fluorescent CgA₁₋₆₀ were obtained. The peak containing TRITC-CgA₁₋₆₀ modified in a 1:1 stoichiometry, as determined by electrospray mass spectrometry, was used for the experiments. FITC-CgA₁₋₆₀ was prepared accordingly.

Analytical Gel Filtration

Gel filtration of purified CgA was performed at 4 °C using an FPLC system (Pharmacia) equipped with a Superdex 200 HR column (10 × 300 mm) run with a flow rate of 0.7 ml/min. The buffers used for the preincubation and incubation of the samples prior to FPLC and for the FPLC itself were 100 mM NaCl, 1 mM EDTA, and either 50 mM sodium phosphate (pH 7.4 and 6.4) or 50 mM sodium acetate (pH 5.4) as indicated in the legend to Fig. 1. DTT and CgA peptides were added to the buffer as indicated in the legend to Fig. 1. The elution of proteins was monitored by UV absorption at 280 nm.

Sucrose Gradient Centrifugation

A solution (150 μl) containing either purified TRITC-CgA or a mixture of TRITC-CgA plus CgA₁₋₆₀ was layered on top of a 4-ml linear 5–20% (w/v) sucrose gradient and centrifuged at 4 °C in a Beckman SW60 rotor for 15 h at 60,000 rpm. Both sample and sucrose gradient contained 100 mM NaCl, 1 mM EDTA, and either 50 mM sodium phosphate (pH 6.4 for CgA, pH 7.4 for marker proteins) or 50 mM sodium acetate (pH 5.4 for CgA). In the case of centrifugation of the TRITC-CgA/CgA₁₋₆₀ mixture, the sucrose gradient in addition contained 30 μM CgA₁₋₆₀. Fractions (170 μl) were collected from the top of the gradient and analyzed in a Shimadzu FR 1502 spectrofluorometer (for TRITC-CgA) or by SDS-PAGE followed by Coomassie Blue staining (for marker proteins). The *S* values and molecular masses of the marker proteins (23) were plotted as a function of their migration from the top of the sucrose gradient in a linear and semilogarithmic plot, respectively. For each condition, the apparent *S* value and apparent molecular mass of TRITC-CgA was calculated using linear regression.

Fluorescence Resonance Energy Transfer (FRET) Studies

Determination of Dissociation Constants

The FITC-CgA or FITC-CgA₁₋₆₀ donor and the TRITC-CgA or TRITC-CgA₁₋₆₀ acceptor were dissolved in FRET buffer (50 mM sodium phosphate, pH 7.4 or 6.4, and 0.5 mg/ml BSA). The molar ratio between donor and acceptor was usually 1:4 (see figure legends). The total concentration of donor plus acceptor ranged from 10 nM to 3 μM. For the unquenched controls, the TRITC-CgA or TRITC-CgA₁₋₆₀ was replaced by the corresponding amounts of unlabeled CgA or CgA₁₋₆₀ plus TRITC-ethanolamine. Fluorescence measurements were performed using a Shimadzu FR 1502 spectrofluorometer. Fluorescence was excited at a wavelength of 485 nm, and the emission spectrum was recorded from 450 to 650 nm. The intensity of the fluorescein emission peak at 516 nm was used for subsequent analysis of the data.

The relative amount of energy transfer (*E*) is given by the difference between unquenched (*U*) and quenched (*Q*) donor fluorescence intensity, normalized to the unquenched donor fluorescence intensity at the same total concentration, according to the equation,

$$E = (U - Q)/U \quad (\text{Eq. 1})$$

The concentration dependence of the energy transfer from a donor *X* to a homologous acceptor in a monomer-dimer equilibrium, $X + X \rightleftharpoons X_2$ is given by the equation,

$$E = E_{\text{transfer}}/f_{\text{stat}} \times X_D/X_T \quad (\text{Eq. 2})$$

where E_{transfer} is the transfer efficiency for a donor-acceptor pair X_2 , X_D is the amount of *X* in dimeric form, and X_T is the total amount of *X*. Accordingly, X_D/X_T gives a value between 0 (100% monomeric) and 1 (100% dimeric).

f_{stat} is a factor accounting for the statistics of formation of donor-donor, donor-acceptor, and acceptor-acceptor pairs, considering that the fluorescence of donor-donor pairs is not quenched. f_{stat} is calculated according to the equation,

$$f_{\text{stat}} = (n + 1)/n \quad (\text{Eq. 3})$$

with *n* corresponding to the molar ratio of acceptor to donor.

The term X_D/X_T can be expressed as a function of the dissociation constant K_D and the total concentration

$$\frac{X_D}{X_T} = 1 - \frac{\sqrt{1/2K_D(X_T + 1/8K_D)} - 1/4K_D}{X_T} \quad (\text{Eq. 4})$$

which gives the equation,

$$E = \frac{E_{\text{transfer}}}{f_{\text{stat}}} \times \left(1 - \frac{\sqrt{1/2K_D(X_T + 1/8K_D)} - 1/4K_D}{X_T} \right) \quad (\text{Eq. 5})$$

Equation 5 was used to obtain the values for the FRET efficiency E_{transfer} and the dissociation constant of the dimer K_D from the energy transfer values *E* (Eq. 1), using least square fitting.

Determination of Kinetic Constants

Dissociation of the Dimer—A relatively concentrated mixture of FITC-CgA and TRITC-CgA (ratio 1:4, total concentration 9 μM in FRET buffer), present in a cuvette placed in the spectrofluorometer, was

rapidly mixed with 50–200 volumes of FRET buffer. The dissociation of the dimer was immediately monitored at 25 °C by measuring the time-dependent increase of the donor fluorescence at 516 nm.

The total increase in donor fluorescence intensity caused by dimer dissociation is given as the difference between the donor fluorescence intensity I_{eq} in the equilibrium and the donor fluorescence intensity I_0 measured immediately after mixing. The kinetics of the increase in donor fluorescence and hence the dissociation of the dimer can be described by a first order rate equation,

$$I_{\text{eq}} - I_t = (I_{\text{eq}} - I_0) \times e^{-k_1 t} \quad (\text{Eq. 6})$$

expressed alternatively as the equation,

$$\ln(I_{\text{eq}} - I_t) = \ln(I_{\text{eq}} - I_0) - k_1 t \quad (\text{Eq. 7})$$

with I_t being the donor fluorescence intensity at the time t .

The experimental data were plotted according to Equation 7, and the first order rate constant of dissociation, k_1 , was determined by linear regression of the data points obtained during the first six seconds after mixing.

Formation of Dimers—A mixture (1.39 ml) of FITC-CgA and TRITC-CgA (ratio 1:1, total concentration 70–210 nM in 10 mM sodium phosphate, pH 7.9, 0.5 mg/ml BSA) was pipetted into a cuvette placed in the spectrofluorometer. This solution was rapidly mixed with 110 μ l containing 0.5 M NaH_2PO_4 and 0.5 mg/ml BSA, yielding a final buffer composition of 50 mM sodium phosphate, pH 6.4. The formation of dimers was immediately monitored at 25 °C by measuring the time-dependent decrease in the donor fluorescence intensity at 516 nm.

The slope dI/dt of the curve obtained is proportional to the reaction rate v . The initial dI/dt was used to calculate the rate of consumption of monomeric donor, which equals the rate of formation of donor-acceptor dimer, according to the equation,

$$v = dI/dt \times [\text{donor}]_0 / I_0 \times f_{\text{stat}} / E_{\text{transfer}} \quad (\text{Eq. 8})$$

where $[\text{donor}]_0$ is the concentration of FITC-CgA after mixing. The second order rate constant of dimer formation, k_2 , was calculated according to the equation,

$$k_2 = v / ([\text{donor}][\text{acceptor}]) \quad (\text{Eq. 9})$$

Miscellaneous Procedures

Protein in solution was determined by the Bradford assay (22), using BSA as a standard. Proteins fixed and Coomassie Blue-stained in gels were quantitated by densitometric scanning.

RESULTS

The N-terminal Domain of CgA Containing the Disulfide-bonded Loop Has an Essential Role in Homodimerization—To investigate a possible role of the N-terminal domain of CgA in homo-oligomerization, we used full-length CgA and CgA_{1–60}, which extends 22 amino acid residues beyond the disulfide-bonded loop (24, 25). CgA obtained from bovine chromaffin granules by lysis at pH 6.4 in the presence of 20 mM calcium (which removes CgB by precipitation) was either purified to homogeneity by sequential anion exchange and gel filtration FPLC or subjected to limited proteolysis by V-8 protease (which cleaves the protein at Glu⁶⁰) followed by purification of CgA_{1–60} by sequential anion exchange and reverse phase FPLC. The identity of CgA_{1–60} was verified by N-terminal sequencing (LPVNSP) and matrix-assisted laser desorption/ionization mass spectrometry ($m/z = 6766$, which corresponds well to the predicted mass of disulfide-bonded CgA_{1–60} of 6767).

We first investigated the effect of CgA_{1–60} on the oligomeric state of full-length CgA as revealed by gel filtration. In line with previous observations (26), full-length CgA, which has been shown to be a homodimer at pH 7.5 (27), behaved anomalously upon gel filtration at pH 7.4 (Fig. 1, A–D, *dashed lines*) or pH 6.4 (the luminal pH of the TGN (10)) (Fig. 1, E–H, *dashed lines*), eluting at the position corresponding to a globular protein of 550 kDa, although the molecular mass of a single CgA polypeptide without post-translational modifications is 48 kDa (24). At pH 7.4 (Fig. 1B, *solid line*), and even more so at pH 6.4 (Fig. 1F, *solid line*), the addition of a 10-fold molar excess of

CgA_{1–60} caused a shift in the peak of full-length CgA toward larger elution volumes, corresponding to a 2-fold reduction in apparent molecular mass. Analysis of the eluted material by SDS-PAGE showed that the shifted peak contained both full-length CgA and CgA_{1–60} (Fig. 2). SDS-PAGE under reducing and nonreducing conditions of full-length CgA alone and of a mixture of full-length CgA plus CgA_{1–60} identical to that subjected to gel filtration indicated the absence of any disulfide-linked homo- or hetero-oligomers (data not shown). We conclude that the addition of CgA_{1–60} reduced the amount of homodimeric CgA and resulted in the formation of a heterodimer between full-length CgA and CgA_{1–60}.

We then examined whether the single intramolecular disulfide bond in the N-terminal domain of CgA (17) was required for the dimerization of CgA. After treatment with the thiol-reducing agent DTT (Fig. 1, A and E, *solid lines*), full-length CgA became monomeric, eluting from the gel filtration column at a position very similar to that of the heterodimer between full-length CgA and CgA_{1–60}. Given that the dimers of full-length CgA (27) are not due to intermolecular disulfide bridges (17) (data not shown), we conclude that the disulfide-bonded loop plays a crucial role in the noncovalent dimerization of CgA.

Loop-mediated Homodimerization Is a Prerequisite for Homotetramerization of CgA—Upon gel filtration at pH 5.4 (the luminal pH of mature secretory granules of neuroendocrine cells (28)) (Fig. 1, I–L, *dashed lines*), full-length CgA eluted earlier than at pH 6.4 and 7.4, consistent with CgA being a homotetramer at pH 5.5 (27). Treatment of full-length CgA with DTT at pH 7.4 followed by gel filtration at pH 5.4 resulted in the appearance of a second peak (Fig. 1I, *solid line*). By comparison with monomeric CgA at pH 6.4 (Fig. 1E, *solid line*), this second peak was likely to correspond to monomeric full-length CgA, indicating a tetramer-monomer equilibrium at pH 5.4. No peak was detected in a position expected of a CgA dimer. Similar observations were made after the addition of CgA_{1–60} at pH 5.4. Here, the second peak was likely to correspond to the heterodimer between full-length CgA and CgA_{1–60} (Fig. 1J, *solid line*), indicating a homotetramer-heterodimer equilibrium at pH 5.4. No peak was detected in a position expected of a (CgA-CgA_{1–60})₂ heterotetramer. We conclude that the disulfide-bonded loop is of critical importance in maintaining the homotetrameric state of CgA that exists at pH 5.4.

Homotetramerization of CgA Involves an Interaction of Its C-terminal Domain—When gel filtration of full-length CgA at pH 5.4 was performed in the presence of the synthetic peptide CgA_{406–431}, which corresponds to the C-terminal domain of CgA, a protein complex of smaller size was eluted (Fig. 1K, *solid line*). This complex, however, was larger than the CgA-CgA_{1–60} heterodimer and presumably corresponded to the (CgA-CgA_{406–431})₂ heterotetramer. Upon the addition of both CgA_{1–60} and CgA_{406–431}, full-length CgA was recovered as a peak with a shoulder, which reflected an equilibrium between the (CgA-CgA_{406–431})₂ heterotetramer and a CgA_{1–60}-CgA-CgA_{406–431} heterotrimer, respectively (Fig. 1L, *solid line*). No effect of the CgA_{406–431} peptide, alone or in combination with CgA_{1–60}, was detected at pH 6.4 (Fig. 1, G and H, *solid lines*) and pH 7.4 (Fig. 1, C and D, *solid lines*). We conclude that at pH 5.4, the C-terminal domain of CgA mediates the assembly of CgA homotetramers from CgA homodimers; assembly of the latter depends on the disulfide-bonded loop.

In addition to the above changes in the oligomeric state of CgA, we noticed that the apparent size of full-length CgA in any given oligomeric state decreased upon reduction in pH from pH 7.4 to 5.4. Similar pH-induced shifts in elution volume were observed when full-length CgA was present as monomer

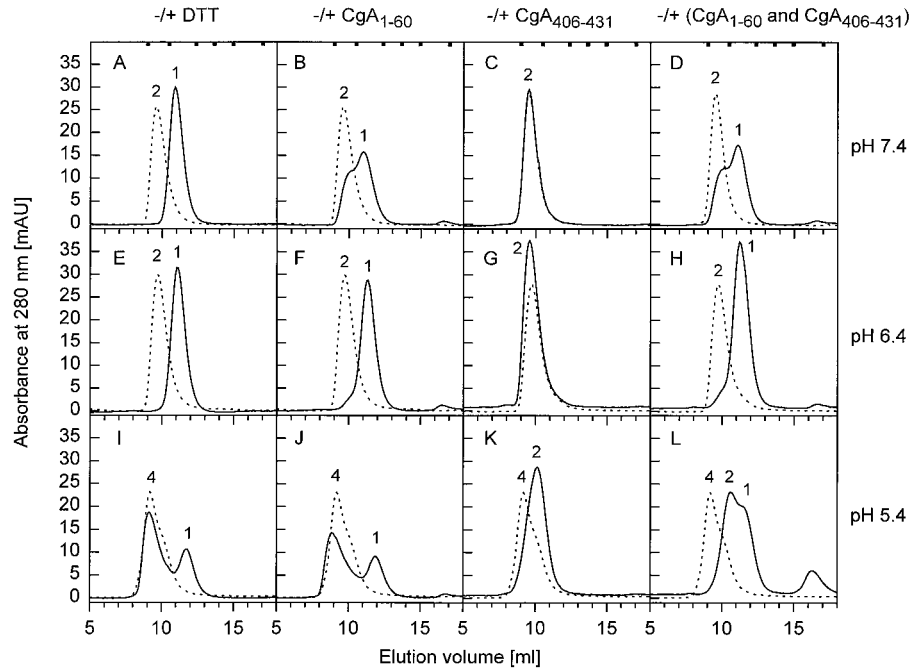


FIG. 1. Gel filtration of CgA under various conditions. Purified CgA ($4 \mu\text{M}$) was incubated at 37°C in the absence (–, *dashed lines*) and presence (+, *solid lines*) of 20 mM DTT (A, E, and I), $40 \mu\text{M}$ CgA_{1–60} (B, F, and J), $400 \mu\text{M}$ CgA_{406–431} (C, G, and K), or $40 \mu\text{M}$ CgA_{1–60} plus $400 \mu\text{M}$ CgA_{406–431} (D, H, and L). Incubations were carried out for 30 min at pH 7.4 (A–D), pH 6.4 (E–H), or pH 5.4 (I–L). Samples containing DTT had been preincubated in the presence of DTT for 30 min at pH 7.4 prior to the 30-min incubation at either pH 7.4, 6.4, or 5.4. After incubation, samples were subjected to gel filtration by FPLC at 4°C using a Superdex 200 HR column, with on-line recording of the absorbance at 280 nm. FPLC was carried out at the same pH and with the same additions as in the incubations, except that DTT was reduced to 5 mM, CgA_{1–60} was omitted, and CgA_{406–431} was reduced to $10 \mu\text{M}$. Numbers above peaks and shoulders indicate the presumptive oligomeric state with respect to full-length CgA and ignore the contribution of CgA_{1–60} and CgA_{406–431} to the oligomers. The small peak at 16–17 ml of elution is due to free CgA_{1–60} (compare Fig. 2), which does not contain tryptophan and tyrosine and therefore contributes little to the absorbance at 280 nm; the relatively high peak at this position in panel L is due to presence of trace amounts of CgA_{1–60} modified by an aromatic group. Note that in panel C the *solid line* and the *dashed line* are exactly superimposed. *Solid squares* at the top of panels A–D indicate the position of elution of marker proteins (from left to right: thyroglobulin, 660 kDa; ferritin, 440 kDa; IgG, 150 kDa; apotransferrin, 81 kDa; ovalbumin, 43 kDa; myoglobin, 18 kDa).

(obtained after DTT treatment; Fig. 1, A, E, and I, *solid lines*), CgA-CgA_{1–60} heterodimer (Fig. 1, B, F, and J, *solid lines*), CgA_{1–60}-CgA-CgA_{406–431} heterotrimer (Fig. 1, D, H, and L, *solid lines*), or (CgA-CgA_{406–431})₂ heterotetramer (Fig. 1, C, G, and K, *solid lines*).

Sedimentation Analysis of CgA Oligomers—To corroborate the changes in the oligomeric state of full-length CgA caused by the addition of CgA_{1–60} and by the reduction of the pH to 5.4, we analyzed the sedimentation of purified full-length CgA upon sucrose gradient centrifugation, using the TRITC-CgA prepared for the FRET analyses described below. At pH 6.4, full-length CgA sedimented with an apparent *S* value of 4.0, corresponding to an apparent molecular mass for a globular protein of 44 kDa (Fig. 3A, *open circles*). Upon centrifugation in the presence of excess CgA_{1–60}, full-length CgA sedimented more slowly, with an apparent *S* value of 3.5, corresponding to an apparent molecular mass for a globular protein of 34 kDa (Fig. 3A, *solid circles*). This change in sedimentation was consistent with the conversion of full-length CgA homodimers into CgA-CgA_{1–60} heterodimers upon the addition of CgA_{1–60} observed in gel filtration (Fig. 1F). At pH 5.4, most (67%) of the full-length CgA sedimented significantly faster than at pH 6.4, being recovered in the pellet and the bottom three fractions of the gradient (apparent *S* value ≥ 7.2 , corresponding to an apparent molecular mass for a globular protein of ≥ 169 kDa; Fig. 3B, *open circles*). This was in line with most of the CgA being a homotetramer at pH 5.4 (27) (Fig. 1J, *dashed line*). A small peak (18% of the TRITC-CgA) was observed in the position of the CgA homodimer (Fig. 3B, *open circles*), consistent with the presence of a small shoulder of homodimeric CgA observed in

gel filtration (Fig. 1J, *dashed line*). The addition of excess CgA_{1–60} reduced the proportion of homotetrameric CgA at the bottom of the gradient from 67 to 54% of total and resulted in the appearance of a peak of full-length CgA in the position of the CgA-CgA_{1–60} heterodimer, which contained 26% of the total full-length CgA in the gradient (Fig. 3B, *solid circles*). This was in line with the conversion of a portion of homotetrameric full-length CgA to the CgA-CgA_{1–60} heterodimer upon the addition of CgA_{1–60} observed in gel filtration, which resulted in a 2:1 ratio between these two oligomers (Fig. 1J, *solid line*).

The N-terminal Domain of CgA Forms Homodimers—The above gel filtration studies showed that the N-terminal domain of CgA containing the disulfide-bonded loop is necessary for the dimerization of CgA but did not provide information as to the underlying mechanism. Two possibilities were most likely: (i) the binding of two N-terminal domains to each other or (ii) the binding of one N-terminal domain to another domain of CgA. To investigate the first possibility directly, we used FRET (29). In this method, the fluorescence energy of an excited donor fluorophore is transferred to an appropriate acceptor if the latter is in sufficient spatial proximity, resulting in a quench of donor fluorescence. We used fluorescein as donor fluorophore and tetramethylrhodamine as acceptor and prepared FITC-labeled CgA_{1–60} and TRITC-labeled CgA_{1–60}, respectively, each with a stoichiometry of 1 mol of chromophore/mol of peptide as determined by mass spectrometry. For fluorescein as donor and tetramethylrhodamine as acceptor, half-maximal FRET occurs at a distance of 5.4 nm between the two chromophores (30). Hence, in a dilute solution of FITC-CgA_{1–60} and TRITC-CgA_{1–}

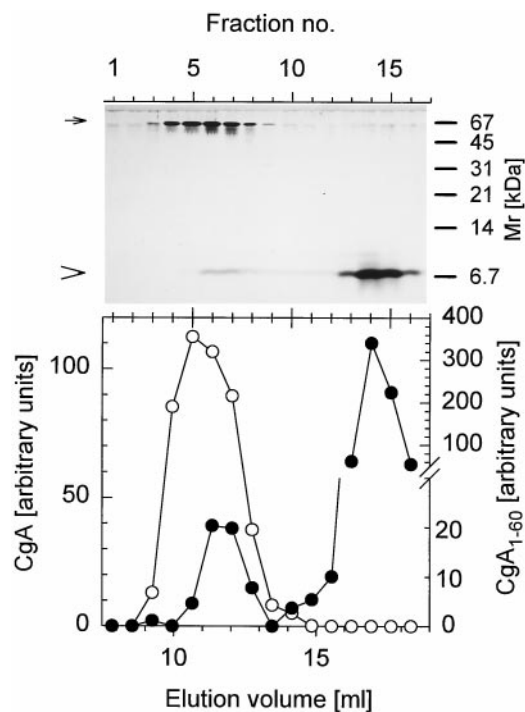


FIG. 2. **CgA₁₋₆₀ binds to monomeric full-length CgA.** Purified CgA (4 μ M) and CgA₁₋₆₀ (40 μ M) were incubated at pH 7.4 and subjected to gel filtration as described in Fig. 1B (solid line). After 7.5 ml of elution, 700- μ l fractions were collected (7.5–8.2 ml of elution = fraction 1). Fractions were analyzed by Tris-Tricine SDS-PAGE followed by Coomassie Blue staining (top). Full-length CgA (arrow) and CgA₁₋₆₀ (arrowhead) are indicated; positions of molecular mass markers are given on the right. Full-length CgA (open circles) and CgA₁₋₆₀ (filled circles) were quantitated (bottom). Note the correspondence between Coomassie Blue-stained CgA (peak in fractions 4–7, 9.5–12 ml of elution) and the absorbance shown in Fig. 1B (solid line, peak at 9.5–12 ml of elution). To accommodate the peak of free CgA₁₋₆₀ (fractions 14 and 15, 16.6 ml of elution) in the bottom panel, the ordinate scale has been adjusted.

60, FRET will only occur if the two labeled peptides are brought together by a binding interaction, *i.e.* dimerize.

Fig. 4 shows the fluorescence spectrum upon excitation at 485 nm of FITC-CgA₁₋₆₀ in the presence of either unlabeled CgA₁₋₆₀ plus free TRITC-ethanolamine (unquenched, line with arrow) or TRITC-CgA₁₋₆₀ (quenched, line with open arrowhead). In the presence of 0.64 μ M TRITC-CgA₁₋₆₀, fluorescence at 516 nm emitted from 0.16 μ M FITC-CgA₁₋₆₀ was quenched by 67% (FRET value of 0.67).

The FRET values showed a concentration dependence consistent with a reversible dimerization of CgA₁₋₆₀ (Fig. 5A, open circles). If this dimerization reflected the mechanism underlying the dimerization of full-length CgA, the reduction of the disulfide bridge should suppress the dimerization of CgA₁₋₆₀ as it did for full-length CgA in the gel filtration experiments. Indeed, no FRET between FITC-CgA₁₋₆₀ and TRITC-CgA₁₋₆₀ was detectable after treatment with DTT at pH 7.4 (Fig. 5A, solid circles) or pH 6.4 (data not shown). The lack of FRET was not due to the loss of the chromophore from either labeled CgA₁₋₆₀ caused by the DTT treatment, as indicated by SDS-PAGE of the peptides followed by analysis of the fluorescence (data not shown).

The FRET values obtained at various concentrations of labeled CgA₁₋₆₀ at pH 7.4 and pH 6.4 (Fig. 5B) were used to calculate the equilibrium binding constants of dimerization (K_D), which were found to be 85 and 20 nM, respectively (Table I). Extrapolation of the individual FRET values yielded an E_{transfer} value of ≥ 0.9 , indicating that the distance between the

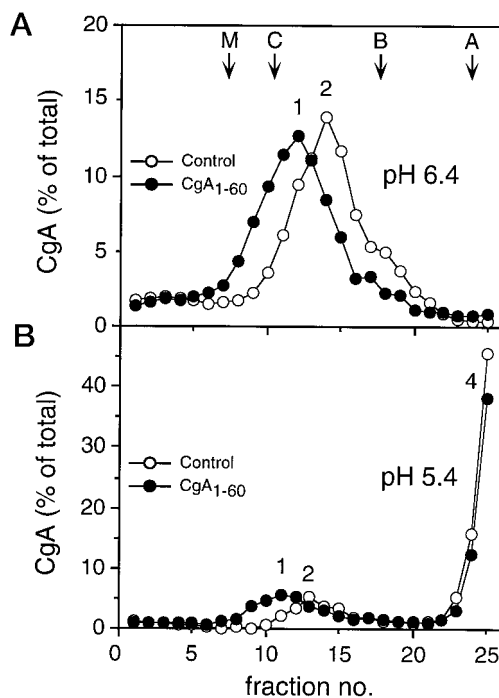


FIG. 3. **Sedimentation analysis of CgA.** Purified TRITC-CgA (3.3 μ M) was subjected to sucrose gradient centrifugation in the absence (Control, open circles) or presence (CgA₁₋₆₀, solid circles) of CgA₁₋₆₀ (177 μ M in the sample, 30 μ M in the gradient) at either pH 6.4 (A) or pH 5.4 (B). Fluorescent TRITC-CgA in the fractions (fraction 1, top of gradient) is expressed as a percentage of the total recovered in the sum of the gradient fractions (pH 6.4 control, 1359 fluorescence intensity units (FIU); pH 6.4 CgA₁₋₆₀, 1830 FIU; pH 5.4 control, 1051 FIU; pH 5.4 CgA₁₋₆₀, 1346 FIU). Note that the pellet of TRITC-CgA was resuspended in the bottom fraction (number 25). Arrowheads indicate the position of marker proteins (M, horse myoglobin (18 kDa, $S = 1.97$); C, bovine erythrocyte carboanhydrase (29 kDa, $S = 2.8$); B, bovine serum albumin (66 kDa, $S = 4.31$); A, yeast alcohol dehydrogenase (150 kDa, $S = 7.61$). Numbers above peaks indicate the presumptive oligomeric state with respect to full-length CgA and ignore the contribution of CgA₁₋₆₀ to the CgA-CgA₁₋₆₀ heterodimer.

two chromophores in the CgA₁₋₆₀ dimer was significantly less than 5.4 nm.

FRET Analysis of the Dimerization of Full-length CgA—We extended the FRET analysis to full-length CgA to obtain equilibrium binding constants and to corroborate the effects, observed in gel filtration, of DTT, CgA₁₋₆₀, and CgA₄₀₆₋₄₃₁ on the dimerization of full-length CgA. Purified full-length CgA was conjugated with either FITC or TRITC, and labeled dimeric CgA was isolated at pH 7.4. The molar ratio of chromophore to protein in either labeled CgA was $\sim 3:1$. As with CgA₁₋₆₀, the binding constant of full-length CgA dimerization (calculated from the individual FRET values; Fig. 6A) was lower at pH 6.4 (214 nM) than at pH 7.4 (1.6 μ M) (Table I). However, half-maximal dimerization of full-length CgA occurred at a 10–20-fold higher concentration than that of CgA₁₋₆₀. Consistent with the results of gel filtration, DTT treatment (Fig. 6C) or the addition of excess unlabeled CgA₁₋₆₀ (Fig. 6B), but not unlabeled CgA₄₀₆₋₄₃₁ (Fig. 6B), abolished most of the FRET between full-length CgA at pH 6.4. We conclude that the N-terminal domain of CgA is the major determinant for its dimerization and that the dimerization mediated by this domain is promoted at mildly acidic pH, a characteristic feature of the lumen of the TGN (10), where sorting to the regulated pathway of protein secretion begins (1, 3).

Kinetics of CgA Dimer Dissociation and Monomer Association—FRET occurs in the nanosecond range and therefore allows measurement of protein interaction kinetics that are too

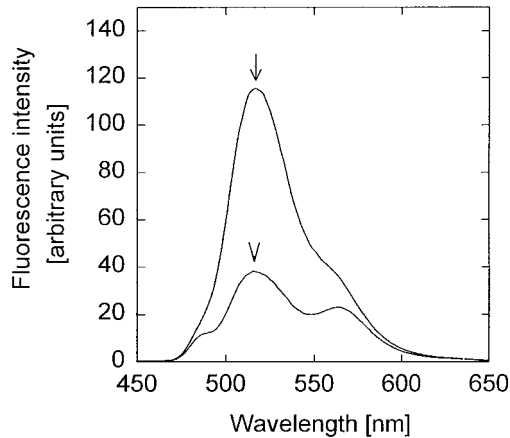


FIG. 4. **FRET between FITC-CgA₁₋₆₀ and TRITC-CgA₁₋₆₀.** FITC-CgA₁₋₆₀ (0.16 μ M) was incubated at pH 7.4 with a mixture of CgA₁₋₆₀ (0.64 μ M) and TRITC-ethanolamine (0.64 μ M) (line with arrow) or with TRITC-CgA₁₋₆₀ (0.64 μ M) (line with open arrowhead). The fluorescence emission spectrum was obtained using an excitation wave length of 485 nm; fluorescence intensity is given as arbitrary units. The arrow and open arrowhead indicate the intensity of FITC fluorescence at 516 nm in the presence of CgA₁₋₆₀ plus TRITC-ethanolamine (unquenched, *U*) and TRITC-CgA₁₋₆₀ (quenched, *Q*), respectively; the energy transfer (*E*) values shown in Figs. 4 and 5 were obtained according to the equation $E = (U - Q)/U$.

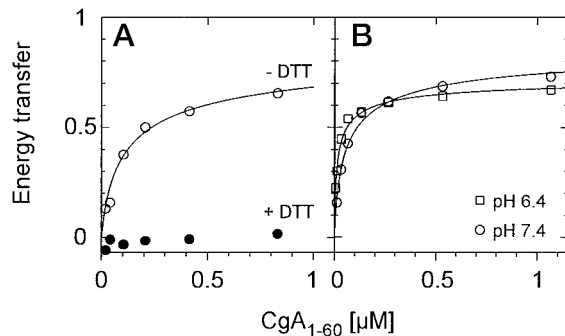


FIG. 5. **FRET analysis of CgA₁₋₆₀ dimerization.** Stock mixtures containing FITC-CgA₁₋₆₀ (0.6 μ M) and either TRITC-CgA₁₋₆₀ (2.4 μ M) (for the determination of the quenched fluorescence) or CgA₁₋₆₀ (2.4 μ M) plus TRITC-ethanolamine (2.4 μ M) (for the determination of the unquenched fluorescence) were diluted to the indicated concentration (values on the abscissas refer to the sum of FITC-CgA₁₋₆₀ and TRITC-CgA₁₋₆₀ concentration) and incubated for 30 min at 37 °C, and the binding of FITC-CgA₁₋₆₀ to TRITC-CgA₁₋₆₀ was determined by FRET analysis as described in Fig. 4, under the following conditions. *A*, binding of FITC-CgA₁₋₆₀ to TRITC-CgA₁₋₆₀ at pH 7.4 in the absence (open circles) and presence (filled circles) of DTT. For DTT treatment, an aliquot of each stock mixture was preincubated for 15 min at 37 °C in the presence of 25 mM DTT, and the buffer for dilution contained 5 mM DTT. *B*, binding of FITC-CgA₁₋₆₀ to TRITC-CgA₁₋₆₀ at pH 7.4 (open circles) and pH 6.4 (open squares). The curves shown were the result of least square fitting to the individual FRET values using Equation 5, which describes a monomer-dimer equilibrium.

fast to be easily determined with conventional biochemical methods. The disulfide-bonded loop of the chromogranins is essential for sorting from the TGN to secretory granules (11), presumably because this process requires chromogranin dimerization. Given that the transit time of chromogranins through the TGN, *i.e.* exposure to the mildly acidic pH that strongly promotes the loop-mediated dimerization, is at most a few minutes (31), it was therefore important to determine whether the kinetics of loop-mediated CgA association would be fast enough to allow dimerization to occur during transit through the TGN.

Since the CgA monomer-dimer equilibrium constant (K_D) is known (Table I) (27), the rate constant of CgA monomer association (k_2) can be calculated from the rate constant of CgA dimer dissociation (k_1) according to the equation, $K_D = k_1/k_2$. To determine the kinetics of dissociation of the CgA dimer, a mixture containing FITC-CgA plus TRITC-CgA at a concentration ~ 4 times (pH 7.4) or ~ 50 times (pH 6.4) higher than the respective K_D value was rapidly diluted 200- or 400-fold and subjected to FRET analysis. The resulting dissociation of the CgA dimer to reach the new equilibrium concentration gave rise to an increase in fluorescence, shown for pH 6.4 and a 200-fold dilution in Fig. 7. This increase followed a first order reaction. The fluorescence values were used to calculate the k_1 and the $t_{1/2}$ of the CgA dimer. It was found that the dimer quickly dissociates, with a half-life of 32 s at pH 6.4 and 11 s at pH 7.4 and 25 °C (Table I). The k_1 values were then used to calculate the k_2 values (Table I, asterisks).

A second approach to determine the rate constant of CgA monomer association is to measure the kinetics of its dimerization. For this purpose, we took advantage of the increase in affinity between CgA monomers upon reduction of pH. A mixture containing FITC-CgA plus TRITC-CgA at a concentration of $< 1/10$ the K_D at pH 7.4 and in the range of the K_D at pH 6.4 was rapidly brought from pH 7.9 (mostly monomeric CgA) to a pH of 6.4 to allow dimerization and subjected to FRET analysis. After an immediate drop in fluorescence due to the smaller absorption coefficient of fluorescein at acidic pH (not shown), a decrease in fluorescence over time, corresponding to the formation of CgA dimers, was observed (Fig. 8). This decrease was used to determine the second order rate constant of dimer formation (k_2), which was found to be $1.3 \times 10^5 \text{ s}^{-1} \text{ M}^{-1}$ (pH 6.4, 25 °C), a value in agreement with the k_2 value calculated from the k_1 and K_D values (Table I).

DISCUSSION

The Oligomeric Structure of CgA—Our results, obtained by gel filtration, sedimentation, and FRET analyses, show that the two highly conserved domains of CgA, the N-terminal disulfide-bonded loop and the C-terminal amphipathic α -helix, are of critical importance for the homo-oligomerization of the protein. The N-terminal disulfide-bonded loop is both necessary and sufficient for the homodimerization that occurs at pH 7.4

TABLE I

Equilibrium binding constants and kinetic constants of dimerization of full-length CgA and CgA₁₋₆₀ as determined by FRET analysis

The equilibrium binding constants, K_D , were determined according to Equation 5, and the rate constants of association, k_1 , were determined according to Equation 7. Values for $t_{1/2}$ were calculated from the mean k_1 values according to $t_{1/2} = \ln 2/k_1$. The rate constants of association of CgA monomers, k_2 , were either determined experimentally according to Equation 9 or calculated from the mean k_1 and K_D values according to $k_2 = k_1/K_D$ (asterisks). The number of experiments is given in parentheses. Either the variation of the individual values from the mean ($n = 2$) or the S.D. ($n = 3$) is given. The kinetic constants for CgA₁₋₆₀ were not determined (ND); they were too fast to be determined reliably with the monitoring system available.

	pH 7.4				pH 6.4			
	K_D	k_1	$t_{1/2}$	k_2	K_D	k_1	$t_{1/2}$	k_2
	nM	$\text{s}^{-1} \times 10^2$	s	$\text{s}^{-1} \text{ M}^{-1} \times 10^{-5}$	nM	$\text{s}^{-1} \times 10^2$	s	$\text{s}^{-1} \text{ M}^{-1} \times 10^{-5}$
CgA	1600 \pm 900 (2)	6.6 \pm 0.6 (2)	10.5	0.4*	214 \pm 7 (2)	2.2 \pm 0.1 (2)	32	1.3 \pm 0.3 (3)
CgA ₁₋₆₀	85 \pm 4 (2)	ND	ND	ND	19.5 \pm 0.5 (2)	ND	ND	1.0*

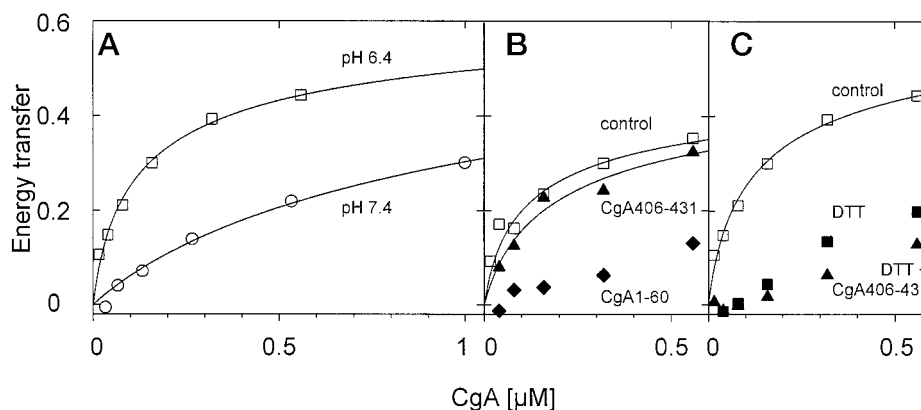


FIG. 6. **FRET analysis of full-length CgA dimerization.** Stock mixtures containing full-length FITC-CgA ($0.2 \mu\text{M}$) and either full-length TRITC-CgA ($0.8 \mu\text{M}$) (for the determination of the quenched fluorescence) or full-length CgA ($0.8 \mu\text{M}$) plus TRITC-ethanolamine ($0.8 \mu\text{M}$) (for the determination of the unquenched fluorescence) were diluted to the indicated concentration (values on the *abscissas* refer to the sum of full-length FITC-CgA and full-length TRITC-CgA concentration) and incubated for 30 min at 37°C , and the binding of full-length FITC-CgA to full-length TRITC-CgA was determined by FRET analysis as described in Fig. 4 under the following conditions. *A*, binding of full-length FITC-CgA to full-length TRITC-CgA at pH 7.4 (*open circles*) and pH 6.4 (*open squares*). *B*, binding of full-length FITC-CgA to full-length TRITC-CgA at pH 6.4 in the absence (*control*, *open squares*) and presence of $10 \mu\text{M}$ CgA₄₀₆₋₄₃₁ (*filled triangles*) or $10 \mu\text{M}$ CgA₁₋₆₀ (*filled diamonds*). *C*, binding of full-length FITC-CgA to full-length TRITC-CgA at pH 6.4 in the absence (*control*, *open squares*) and presence of DTT (*filled squares*) or DTT plus $10 \mu\text{M}$ CgA₄₀₆₋₄₃₁ (*filled triangles*). For DTT treatment, 7-fold concentrated stock mixtures were preincubated at pH 7.4 for 30 min at 37°C in the presence of 45 mM DTT, and the pH 6.4 buffer for dilution contained DTT to yield a concentration of 5 mM after dilution. The curves shown were the result of least square fitting to the individual FRET values using Equation 5, which describes a monomer-dimer equilibrium.

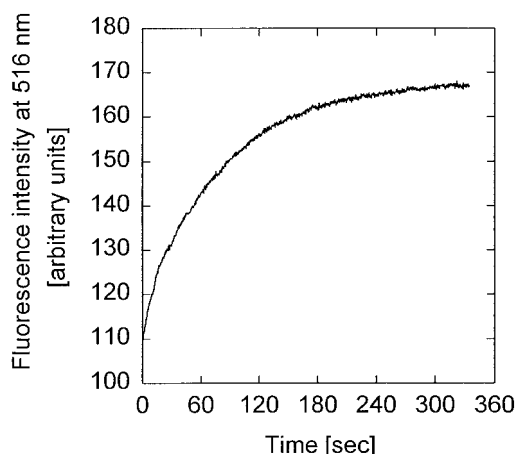


FIG. 7. **Dissociation kinetics of full-length CgA dimers.** A mixture of full-length FITC-CgA ($1.8 \mu\text{M}$) and full-length TRITC-CgA ($7.2 \mu\text{M}$) was rapidly diluted 200-fold at pH 6.4, followed by immediate recording of the intensity of FITC fluorescence at 516 nm using an excitation wave length of 485 nm .

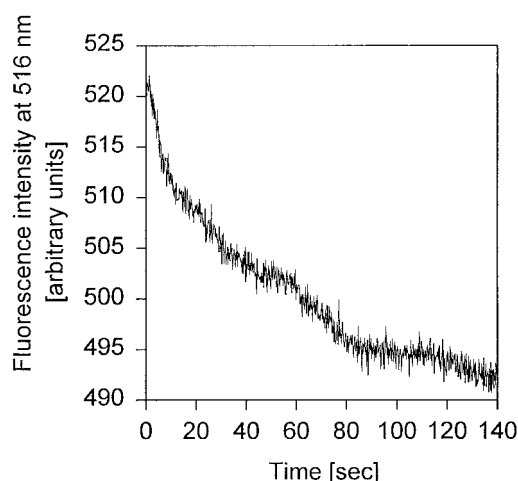


FIG. 8. **Association kinetics of full-length CgA.** A 1:1 mixture of full-length FITC-CgA and full-length TRITC-CgA at pH 7.9 was rapidly brought to pH 6.4 with minimal dilution (90 nM final concentration of either CgA), followed by immediate recording of the intensity of FITC fluorescence at 516 nm using an excitation wave length of 485 nm .

and 6.4 (Fig. 9B), the pH values in the lumen of the secretory pathway from the endoplasmic reticulum (pH 7.4) to the immature secretory granule (pH 6.4) (32). In contrast, the C-terminal amphipathic α -helix showed no detectable (using gel filtration) or only a very minor (using FRET, Fig. 6, *B* and *C*, *triangles*) contribution to the homodimerization of CgA at pH 7.4 and 6.4. Previously, Yoo and Lewis (33) proposed that the C-terminal amphipathic α -helix is the primary domain of CgA mediating the homodimerization at pH 7.5 and homotetramerization at pH 5.5. This conclusion was based on the oligomerization behavior of synthetic peptides corresponding to specific segments of CgA. The apparent disagreement between the previous (33) and our present findings can be explained by the fact that the interaction mediated by the N-terminal disulfide-bonded loop is critically dependent on the oxidized state of the two cysteine residues. The N-terminal synthetic peptide used by Yoo and Lewis (33) did not include these critical two cysteines and, hence, could not adopt a conformation allowing

dimer formation. Furthermore, the binding energy of dimerization measured by Yoo and Lewis for the C-terminal peptide (33) was much smaller than that for full-length CgA (27) and therefore insufficient to account for the dimerization of the latter. In contrast, in our hands, the affinity for homodimerization of the N-terminal disulfide-bonded loop was much larger than that of full-length CgA and hence sufficient to account for the dimerization of full-length CgA.

At pH 5.4, the pH value of mature secretory granules of neuroendocrine cells (28), the intermolecular interactions leading to CgA oligomerization are more complex, involving both the N- and C-terminal domains. Our data support a homotetrameric structure at this pH (Fig. 9C), consistent with previous findings (27). In the formation of the tetramer, the interactions mediated by the N- and C-terminal domains behave in a cooperative manner, with the N-terminal one being a prerequisite for efficient interaction via the C-terminal domain. The follow-

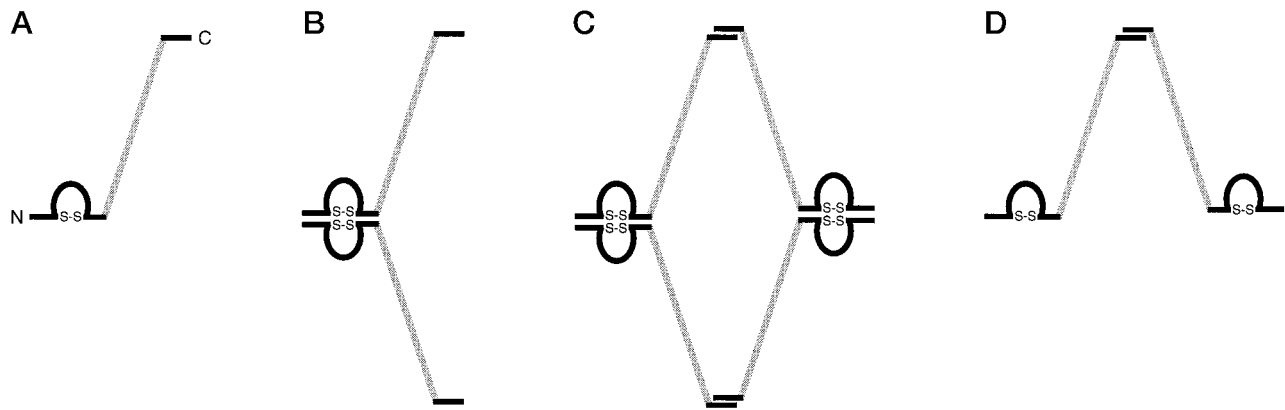


FIG. 9. **Oligomeric states of full-length CgA.** The N-terminal domain containing the disulfide-bonded loop and the C-terminal domain are shown in *black*, and the rest of the molecule is shown in *gray*. Note that the size of the domains is not drawn to scale. *A*, CgA monomer. *B*, CgA dimer, as observed at pH 7.4 and 6.4. Dimerization is mediated by a single homophilic interaction between the N-terminal disulfide-bonded loops and is dependent on the presence of the disulfide bond. *C*, CgA tetramer, as observed at pH 5.4. Formation of tetramers from the dimers shown in *B* requires two parallel C-terminal interactions. *D*, An unstable CgA dimer mediated by a single C-terminal interaction. The fact that this dimer was not observed upon interfering with the homophilic interaction of the N-terminal domain at pH 5.4 (reduction of the disulfide bond or the addition of excess N-terminal peptide) shows the weak and transient nature of a single C-terminal interaction. Dimerization of CgA is shown to result in a more elongated structure relative to the monomer, and tetramerization in a less elongated structure relative to the dimer. This is consistent with the observations that the changes in the behavior of CgA in gel filtration are relatively greater, and those in sedimentation relatively smaller, upon reduction of the disulfide bond or addition of CgA₁₋₆₀ (homodimer dissociation) than upon lowering the pH to 5.4 (homotetramerization). Note that the parallel assembly of the dimerized loop shown in *B* and *C* is hypothetical; an antiparallel assembly is also conceivable.

ing lines of evidence lead to this conclusion. Treatment with DTT or the addition of N-terminal peptide, both of which interfere with the N-terminally mediated interaction between full-length CgA molecules, is sufficient to cause the dissociation of CgA tetramers into monomers. No dimers are seen under these conditions. Dimers, but no monomers, however, are observed when the C-terminally mediated interactions between CgA molecules are blocked by the addition of C-terminal peptide. These observations suggest that C-terminal interactions lead to stable complexes only if they link two preexisting N-terminally bound CgA dimers to one another (Fig. 9C). In this case, the parallel interactions of two pairs of C-terminal domains would contribute twice the binding energy, similar to an antibody binding an oligomeric antigen via its two F_{ab} domains. Another indication for the greater stability of the N-terminal than the C-terminal interaction is that upon gel filtration of CgA, the dissociation of tetrameric CgA into dimers was observed only if the C-terminal peptide was added to both the sample and the running buffer, demonstrating the relatively weak and transient nature of a single C-terminal interaction. In contrast, the dissociation of oligomeric CgA into monomers was observed already if the N-terminal peptide was added to the sample only, showing that a single N-terminal interaction provides sufficient binding energy to give stable complexes.

Dimerization of CgA and Sorting—The N-terminal disulfide-bonded loop is not a feature exclusive to CgA. A highly homologous domain is also found in CgB (17). In PC12 cells, which express CgB but not CgA, reduction of the disulfide bond *in vivo* prevents the sorting of CgB from the TGN into immature secretory granules and results in its exit from the TGN in constitutive secretory vesicles (11). The sorting of secretogranin II, a member of the granin family devoid of cysteine residues (4), was unaffected by the reductive treatment (11). These observations indicated that the disulfide-bonded loop of CgB, and by analogy that of CgA, is necessary for sorting of the chromogranins (11). Together with the present finding that the disulfide-bonded loop mediates the formation of homodimers, we are left with two possible explanations. First, two distinct structural motifs are necessary for dimer formation and sorting, and both are localized to the disulfide-bonded loop. Open-

ing the loop by reduction would independently disturb both dimerization and sorting. This possibility seems unlikely, since the 22-amino acid residue-containing loop is presumably too small to encompass two structural motifs capable of binding to their interaction partners simultaneously. Second, the disulfide-bonded loop is required for sorting of chromogranins because the homodimerization mediated by this structural motif is essential for sorting to occur, a possibility that we favor.

How would the loop-mediated homodimerization of the chromogranins have an essential role in sorting? We would like to discuss this question with respect to the two principal levels of the sorting process in the TGN: (i) the segregation of constitutive and regulated secretory cargo from one another in the lumen of the TGN and (ii) the interaction of regulated secretory cargo with membrane components in the TGN. As to the first level, segregation of regulated from constitutive secretory cargo is thought to be achieved by milieu-induced selective aggregation of the former (7), followed by the exit from the TGN of aggregated secretory proteins in immature secretory granules and of soluble secretory proteins in constitutive secretory vesicles (3). In cells with a very high sorting efficiency such as PC12 cells, this implies that for any given regulated secretory protein, the vast majority of molecules undergoes aggregation during passage through the TGN. Any delay in aggregation during this passage, *i.e.* a $t_{1/2}$ of aggregate formation approaching that of exit in constitutive secretory vesicles, would lead to substantial missorting of the regulated secretory protein. It is conceivable that the loop-mediated dimerization of CgB, although not a prerequisite for its calcium- and low pH-induced aggregation as such (34), provides the nucleating core units necessary for aggregation to approach completion within the time span available for sorting in the TGN.

As to the second level of sorting, the disulfide-bonded loop may be critical for the interaction of chromogranins with membrane components destined to secretory granules. Both direct and indirect roles of the loop in the membrane binding of the chromogranins are conceivable. One such direct role would be a loop-mediated homodimerization, *i.e.* the binding of the loop of a soluble chromogranin molecule to the loop of a tightly membrane-associated chromogranin molecule (35, 36). Another di-

rect role would be the loop-mediated heterodimerization, *i.e.* the binding of the loop of a soluble chromogranin molecule to a membrane receptor. A precedent for a loop-mediated heterodimerization is provided by the finding that pro-opiomelanocortin binds, via its N-terminal disulfide-bonded loop, to the membrane-associated form of carboxypeptidase E (14). An indirect role of the loop in membrane binding of the chromogranins would be the case if dimers, but not monomers, of soluble chromogranin molecules were able to bind with sufficient affinity to either membrane-associated chromogranin (homophilic interaction) or a membrane receptor (heterophilic interaction).

Dynamics and Compartments of CgA Oligomerization—Newly synthesized CgB is transported to the sorting compartment, the TGN, with a $t_{1/2}$ of ~ 7 min (11). If, as discussed above, loop-mediated dimerization of CgB is essential for sorting, the observation that reduction of the disulfide-bonded loop prevents sorting implies that newly synthesized CgB has dimerized by the time it reaches the TGN. Consistent with this, our results on the kinetics of CgA monomer association as determined by FRET reveal that already at a protein concentration much below that likely to exist in the endoplasmic reticulum (the presumptive site of disulfide bond formation), association is complete within ~ 2 min. At a low estimate for the chromogranin concentration in the endoplasmic reticulum of a neuroendocrine cell, $1 \mu\text{M}$, association would be complete within a few seconds. It is therefore likely that chromogranins already dimerize in the endoplasmic reticulum and are transported to the TGN as dimers.

The CgA dimers are not only formed rapidly, they also exhibit a fast rate of dissociation, resulting in a $t_{1/2}$ for the decay of the dimer of ~ 30 s (at 25°C). This implies that although only a small proportion of the CgA in the secretory pathway exists in monomeric form, there is rapid interconversion between the monomeric and dimeric state. This could be relevant for the interaction of soluble CgA with the membrane discussed above.

Finally, our observation that upon lowering the pH from 6.4 to 5.4, CgA homodimers formed homotetramers via C-terminal interactions is intriguing. Such a change in pH corresponds to the acidification known to occur concomitant with secretory granule maturation in neuroendocrine cells (32). It is tempting to speculate that this form of interaction of CgA molecules is involved in the condensation of the secretory cargo during secretory granule maturation.

Acknowledgments—We thank Dr. R. Frank for synthetic peptides, protein sequencing, and mass spectrometry; Dr. H.-H. Gerdes and members of his group for helpful discussions; and Dr. D. Langosch for helpful comments on the manuscript.

REFERENCES

- Burgess, T. L., and Kelly, R. B. (1987) *Annu. Rev. Cell Biol.* **3**, 243–293
- Arvan, P., and Castle, D. (1992) *Trends Cell Biol.* **2**, 327–331
- Tooze, S. A., Chanut, E., Tooze, J., and Huttner, W. B. (1993) in *Mechanisms of Intracellular Trafficking and Processing of Proproteins* (Peng Loh, Y., ed), pp. 157–177, CRC Press, Inc., Boca Raton, FL
- Gerdes, H.-H., Rosa, P., Phillips, E., Baeuerle, P. A., Frank, R., Argos, P., and Huttner, W. B. (1989) *J. Biol. Chem.* **264**, 12009–12015
- Gorr, S.-U., Shioi, J., and Cohn, D. V. (1989) *Am. J. Physiol.* **257**, E247–E254
- Tooze, J., Kern, H. F., Fuller, S. D., and Howell, K. E. (1989) *J. Cell Biol.* **109**, 35–50
- Chanat, E., and Huttner, W. B. (1991) *J. Cell Biol.* **115**, 1505–1519
- Huttner, W. B., Gerdes, H.-H., and Rosa, P. (1991) *Trends Biochem. Sci.* **16**, 27–30
- Winkler, H., and Fischer-Colbrrie, R. (1992) *Neuroscience* **49**, 497–528
- Anderson, R. G. W., and Orci, L. (1988) *J. Cell Biol.* **106**, 539–543
- Chanat, E., Weiß, U., Huttner, W. B., and Tooze, S. A. (1993) *EMBO J.* **12**, 2159–2168
- Tam, W. W. H., Andreasson, K. I., and Peng Loh, Y. (1993) *Eur. J. Cell Biol.* **62**, 294–306
- Cool, D. R., Fenger, M., Snell, C. R., and Loh, Y. P. (1995) *J. Biol. Chem.* **270**, 8723–8729
- Cool, D. R., Normant, E., Shen, F.-S., Chen, H.-C., Pannell, L., Zhang, Y., and Loh, Y. P. (1997) *Cell* **88**, 73–83
- Shen, F.-S., and Loh, Y. P. (1997) *Proc. Natl. Acad. Sci.* **94**, 5314–5319
- Thiele, C., Gerdes, H.-H., and Huttner, W. B. (1997) *Curr. Biol.* **7**, R496–R500
- Benedum, U. M., Lamouroux, A., Konecki, D. S., Rosa, P., Hille, A., Baeuerle, P. A., Frank, R., Lottspeich, F., Mallet, J., and Huttner, W. B. (1987) *EMBO J.* **6**, 1203–1211
- Pohl, T. M., Phillips, E., Song, K., Gerdes, H.-H., Huttner, W. B., and Rüther, U. (1990) *FEBS Lett.* **262**, 219–224
- Iacangelo, A. L., Grimes, M., and Eiden, L. E. (1991) *Mol. Endocrinol.* **5**, 1651–1660
- Wu, H.-J., Rozansky, D. J., Parmer, R. J., Gill, B. M., and O'Connor, D. T. (1991) *J. Biol. Chem.* **266**, 13130–13134
- Bartlett, S. F., and Smith, A. D. (1974) *Methods Enzymol.* **31**, 379–389
- Bradford, M. M. (1976) *Anal. Biochem.* **72**, 248–254
- Smith, M. H. (1970) in *Handbook of Biochemistry* (Sober, H. A., ed), pp. C3-C25, CRC Press, Inc., Cleveland, OH
- Benedum, U. M., Baeuerle, P. A., Konecki, D. S., Frank, R., Powell, J., Mallet, J., and Huttner, W. B. (1986) *EMBO J.* **5**, 1495–1502
- Iacangelo, A., Affolter, H.-U., Eiden, L. E., Herbert, E., and Grimes, M. (1986) *Nature* **323**, 82–86
- Yoo, S. H., and Albanesi, J. P. (1990) *J. Biol. Chem.* **265**, 14414–14421
- Yoo, S. H., and Lewis, M. S. (1992) *J. Biol. Chem.* **267**, 11236–11241
- Johnson, R. G., Jr. (1987) *Annu. N. Y. Acad. Sci. U. S. A.* **493**, 162–177
- Stryer, L. (1978) *Annu. Rev. Biochem.* **47**, 819–846
- Ullman, E. F., and Khanna, P. L. (1981) *Methods Enzymol.* **74**, 28–60
- Tooze, S. A., and Huttner, W. B. (1990) *Cell* **60**, 837–847
- Urbe, S., Dittie, A., and Tooze, S. A. (1997) *Biochem. J.* **321**, 65–74
- Yoo, S. H., and Lewis, M. S. (1993) *Biochemistry* **32**, 8816–8822
- Chanat, E., Weiß, U., and Huttner, W. B. (1994) *FEBS Lett.* **351**, 225–230
- Settleman, J., Nolan, J., and Angeletti, R. H. (1985) *J. Biol. Chem.* **260**, 1641–1644
- Pimplikar, S. W., and Huttner, W. B. (1992) *J. Biol. Chem.* **267**, 4110–4118